

# Evaluating Initial Integration of Cell-Based Chondrogenic Constructs in Human Osteochondral Explants

**Citation for published version (APA):**

Kleuskens, M. W. A., Crispim, J. F., van Donkelaar, C. C., Janssen, R. P. A., & Ito, K. (2022). Evaluating Initial Integration of Cell-Based Chondrogenic Constructs in Human Osteochondral Explants. *Tissue Engineering. Part C: Methods*, 28(1), 34-44. <https://doi.org/10.1089/ten.TEC.2021.0196>

**Document license:**

TAVERNE

**DOI:**

[10.1089/ten.TEC.2021.0196](https://doi.org/10.1089/ten.TEC.2021.0196)

**Document status and date:**

Published: 01/01/2022

**Document Version:**

Publisher's PDF, also known as Version of Record (includes final page, issue and volume numbers)

**Please check the document version of this publication:**

- A submitted manuscript is the version of the article upon submission and before peer-review. There can be important differences between the submitted version and the official published version of record. People interested in the research are advised to contact the author for the final version of the publication, or visit the DOI to the publisher's website.
- The final author version and the galley proof are versions of the publication after peer review.
- The final published version features the final layout of the paper including the volume, issue and page numbers.

[Link to publication](#)

**General rights**

Copyright and moral rights for the publications made accessible in the public portal are retained by the authors and/or other copyright owners and it is a condition of accessing publications that users recognise and abide by the legal requirements associated with these rights.

- Users may download and print one copy of any publication from the public portal for the purpose of private study or research.
- You may not further distribute the material or use it for any profit-making activity or commercial gain
- You may freely distribute the URL identifying the publication in the public portal.

If the publication is distributed under the terms of Article 25fa of the Dutch Copyright Act, indicated by the "Taverne" license above, please follow below link for the End User Agreement:

[www.tue.nl/taverne](http://www.tue.nl/taverne)

**Take down policy**

If you believe that this document breaches copyright please contact us at:

[openaccess@tue.nl](mailto:openaccess@tue.nl)

providing details and we will investigate your claim.

**METHODS ARTICLE**

---

# Evaluating Initial Integration of Cell-Based Chondrogenic Constructs in Human Osteochondral Explants

Meike W.A. Kleuskens, MSc,<sup>1,i</sup> João F. Crispim, PhD,<sup>1</sup> Corrinus C. van Donkelaar, PhD,<sup>1</sup>  
Rob P.A. Janssen, MD, PhD,<sup>1-3</sup> and Keita Ito, MD, ScD<sup>1</sup>

Integration of an implant with the surrounding tissue is a major challenge in cartilage regeneration. It is usually assessed with *in vivo* animal studies at the end-stage of implant development. To reduce animal experimentation and at the same time increase screening throughput and speed up implant development, this study examined whether integration of allogeneic cell-based implants with the surrounding native cartilage could be demonstrated in an *ex vivo* human osteochondral culture model. Chondrocytes were isolated from smooth cartilage tissue of fresh human tibial plateaus and condyles. They were expanded for 12 days either in three-dimensional spinner flask cultures to generate organoids, or in two-dimensional culture flasks for standard cell expansion. Three implant groups were created (fibrin+organoids, fibrin+cells, and fibrin only) and used to fill a Ø 6 mm full-depth chondral defect created in human osteochondral explants (Ø 10 mm, bone length cut to 4 mm) harvested from a second set of fresh human tibial plateaus. Explants were cultured for 1 or 28 days in a double-chamber culture platform. Histology showed that after 28 days the organoids on the interface of the defect remodeled and merged, and cells migrated through the fibrin glue bridging the space between the organoids and between the organoids and the native cartilage. For both conditions, newly formed tissue rich in proteoglycans and collagen type II was present mainly on the edges and in the corners of the defect. In these matrix-rich areas, cells resided in lacunae and the newly formed tissue integrated with the surrounding native cartilage. Biochemical analysis revealed a statistically significant effect of culture time on glycosaminoglycan (GAG) content, and showed a higher hydroxyproline (HYP) content for organoid-filled implants compared with cell-filled implants at both time-points. This *ex vivo* human osteochondral culture system provides possibilities for exploration and identification of promising implant strategies based on evaluation of integration and matrix production under more controlled experimental conditions than possible *in vivo*.

**Keywords:** articular cartilage, osteochondral, *ex vivo*, integration, explant, organoids

## Impact Statement

Implant integration is a persisting challenge in cartilage regeneration. In this work, initial implant integration could be demonstrated when cartilage organoids or single chondrocytes mixed in fibrin were implanted in a chondral defect in an *ex vivo* human osteochondral explant. This opens possibilities for exploring cartilage treatment options in an *ex vivo* human osteochondral explant and allows for identification of the most promising therapies and cell-based implants for animal studies at an early stage of development. This leads to efficient cell-based implant development and lower development costs, reducing the number of animals needed for experimentation and overcoming interspecies translational issues.

---

<sup>1</sup>Orthopaedic Biomechanics, Department of Biomedical Engineering, Eindhoven University of Technology, The Netherlands.

<sup>2</sup>Department of Orthopaedic Surgery and Trauma, Máxima Medical Center, Eindhoven-Veldhoven, The Netherlands.

<sup>3</sup>Department of Paramedical Sciences, Fontys University of Applied Sciences, Eindhoven, The Netherlands.

<sup>i</sup>ORCID ID (<https://orcid.org/0000-0002-7634-0859>).

## Introduction

**F**OCAL DEFECTS IN ARTICULAR CARTILAGE can be caused by, for example, trauma, overloading, or overweight. The intrinsic repair capacity of articular cartilage is very poor due to its low cell density as well as avascular and aneural nature.<sup>1</sup> If left untreated, focal defects can be painful and might progress to osteoarthritis (OA).

In young patients, treatment currently consists of regenerative therapies, such as microfracture, autologous chondrocyte implantation (ACI), matrix-assisted ACI, or spheroid-based technologies.<sup>2</sup> Although short-term repair yields positive results, in the long term, the fibrocartilage that is eventually formed is mechanically inferior to the surrounding cartilage and degrades over time.<sup>3</sup> Furthermore, the often poor integration of the newly formed tissue with the surrounding cartilage has shown to be a major challenge in cartilage regeneration, resulting in uneven distribution of the load and further deterioration of the tissue surrounding the defect.<sup>4</sup>

Integration of an implant with the surrounding cartilage is mostly assessed with *in vivo* animal studies at the end stage of implant development. Although animal studies assessing safety and efficacy of the implant are required for regulatory approval before clinical trials, they are also often used during implant development. As results obtained in animal models are not always directly translatable to human subjects, this leads to ethical questions regarding the often common use of these expensive models.<sup>5</sup>

To reduce and refine animal experimentation, overcome interspecies translational issues, and at the same time speed up implant development and increase throughput, an *ex vivo* human tissue-based approach would be a valuable tool. The most promising implant strategies can be selected at an early stage, limiting the number of animals needed for evaluation and increasing the chance that a product will make it to the patient.

Recently, a human osteochondral culture model was developed that contains separate chambers for the bone and cartilage tissue. Using this setup, it was shown that the viability and biochemical content of human osteochondral explants obtained from total knee replacement (TKR) surgery could be maintained during 28 days in culture.<sup>6</sup> To adopt this culture model as a method to assess and identify promising implant strategies, it is important that integration of an implant with the surrounding cartilage can be demonstrated.

One of the causes for fibrocartilage formation and poor integration resulting from ACI is chondrocyte dedifferentiation during the two-dimensional (2D) expansion step.<sup>7–9</sup> Dedifferentiated chondrocytes from early passages can be redifferentiated in three-dimensional (3D) cultures.<sup>10</sup> A novel, promising ACI-derived approach based on culturing 2D-expanded autologous chondrocytes in hydrogel-coated wells provided with human serum showed redifferentiation and self-aggregation of the chondrocytes into 3D spheroids.<sup>11–13</sup> However, redifferentiation of the cells to chondrocytes is accompanied by loss of proliferative capacity.<sup>11</sup>

Adding porcine notochordal cell-derived matrix (NCM) to a 3D spinner flask suspension culture of bovine chondrocytes has been shown to provide the chondrocytes with a cartilage-like matrix to attach to while also inducing proliferation and maintenance of the chondrogenic phenotype,

leading to their self-assembly into complex 3D hyaline cartilage structures with a pericellular and territorial matrix (organoids) within 12 days.<sup>14,15</sup> These organoids can fuse together to form a tissue that is rich in collagen type II and proteoglycans, which are important cartilage matrix components. These organoids contain the most important prerequisites for appropriate cartilage formation, but so far, these organoids have not been evaluated in terms of integration with the surrounding cartilage.

Without appropriate integration, implants are doomed to fail due to suboptimal load bearing properties leading to further degeneration of the surrounding tissue.

The aim of this study was to evaluate whether the previously mentioned human osteochondral culture model could be used to demonstrate integration of allogeneic cell-based implants with the surrounding native cartilage. Chondral defects were treated using either human 3D-cultured NCM-containing organoids or 2D-cultured chondrocytes, followed by analysis of integration and matrix production.

## Methods

Chondral defects were created in human osteochondral explants with a smooth cartilage surface, obtained from osteoarthritic joints after TKR surgery. The defects were treated using an allogeneic approach with fibrin gel containing human 3D-cultured NCM-containing organoids, 2D-cultured chondrocytes, or no cells, followed by analysis of integration (defined as the presence of no gap regions between the implant and the native tissue, visualized as bridging by cells and extracellular matrix (ECM) across the gap in histologic sections) and matrix production (Fig. 1).

## Experiment

### Experimental design

**NCM harvest.** Nucleus pulposus tissue was collected from the intervertebral discs from the spines of porcine donors, which were slaughtered for meat consumption (~3 months old,  $n=3$ , obtained from the local abattoir). The tissue was pooled, lyophilized (Labconco, Kansas City, MO), and subsequently pulverized using a microdismembrator (Sartorius, Göttingen, Germany). The pulverized NCM was aliquoted and stored at  $-80^{\circ}\text{C}$  until further use.<sup>14</sup>

**Chondrocyte isolation and culture.** On day 1, a first set of human tibial plateaus and condyles was collected from patients (5 subjects, 2 females and 3 males, aged  $67 \pm 6$  years, range 62–77 years) undergoing TKR surgery at Máxima Medical Centre (Eindhoven, The Netherlands). The usage of this residual tissue for research purposes was approved by the Local Research Committee (METC, no. N16.148) and not subjected to the Medical Research Involving Human Subjects Act.

Full-thickness slices of cartilage were removed from parts of the condyles and tibial plateaus that were covered by smooth cartilage. The slices were minced and digested overnight in chondrocyte digestion mixture (Dulbecco's modified Eagle's medium [DMEM] high glucose [41966; Gibco, Bleiswijk, The Netherlands], 10% fetal bovine serum [FBS; Gibco], 1% penicillin/streptomycin [P/S; Lonza, Basel, Switzerland], 0.15% collagenase 2 [Worthington Biochemical

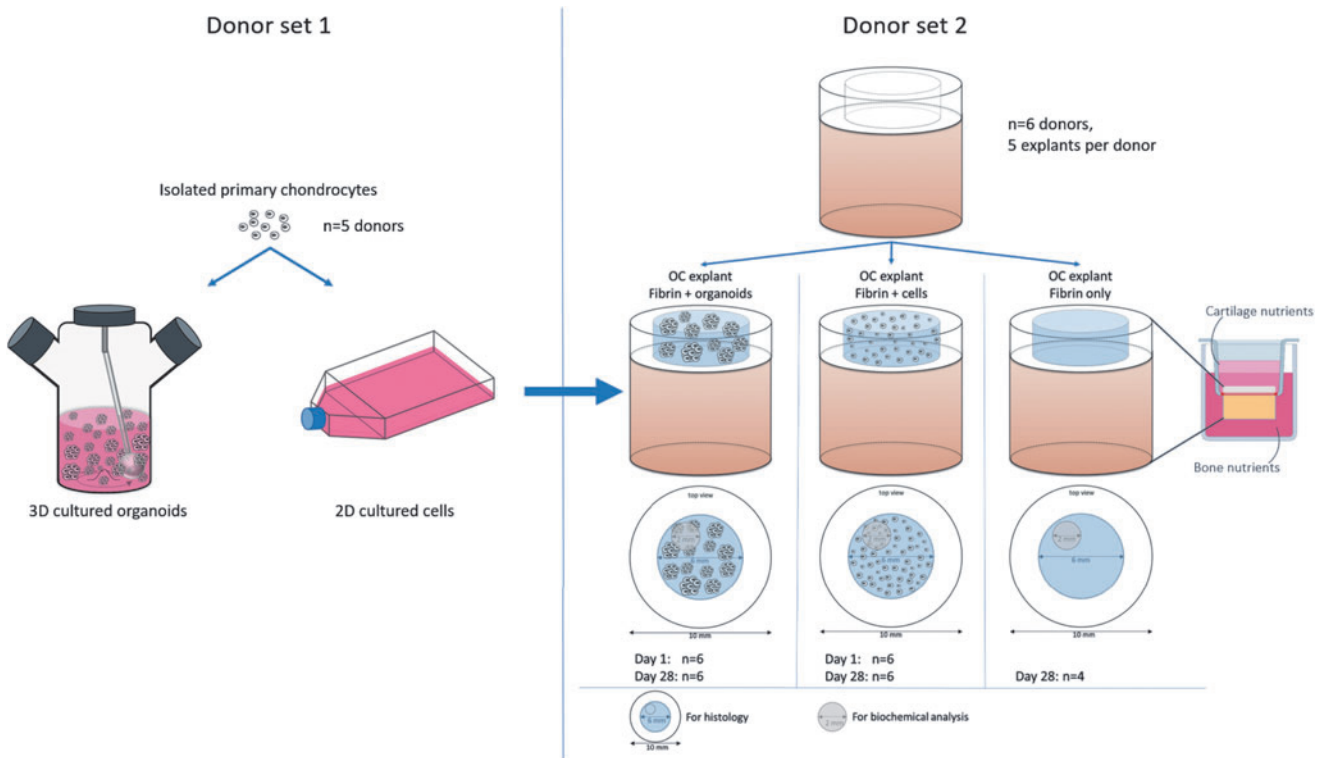


**FIG. 1.** Experimental setup showing the 3D and 2D chondrocyte cultures (*left*) and the explant cultures (*right*). 2D, two-dimensional; 3D, three-dimensional. Color images are available online.

Corporation, Lakewood, NJ], and 0.01% hyaluronidase [Merck KGaA, Darmstadt, Germany]) at 37°C and 5% CO<sub>2</sub>. The cell suspension was strained using a 70 µm cell strainer and chondrocytes were collected.

**3D expansion.** On day 0, for each donor, chondrocytes were seeded into coated spinner flasks (coating: Sigmacote, Sigma-Aldrich; Spinner flask: Wheaton™ Magna-Flex™, DWK Life Sciences, Mainz, Germany) containing 64 mL medium (high-glucose DMEM, 5% FBS, 1% P/S, 10 mM 4-(2-hydroxyethyl)-1-piperazineethanesulfonic acid [Gibco], 1% nonessential amino acids [Gibco], 1% insulin/transferrin/selenium-plus [ITS+ premix; Corning, Fisher Scientific, Landsmeer, NL], and 0.2 mM L-ascorbic acid-2-phosphate [Sigma-Aldrich, Zwijndrecht, The Netherlands]) at a density of  $5 \times 10^4$  viable cells/mL and cultured at an agitation of 60 rpm using a magnetic stirrer (Variomag Biosystem 4 and Biomodul 40B; Thermo Scientific, Waltham, MA) at 37°C, 5% CO<sub>2</sub>, and 2.5% O<sub>2</sub>.

On day 0, the medium was supplemented with NCM (0.25 mg/mL). The NCM was dissolved in DMEM by pipetting up and down until all NCM was dissolved. Then, the other medium components were added. On day 4, half of the culture medium was changed, by removing half of the cell suspension from the spinner flask, spinning down the chondrocytes, resuspending them in suspension culture medium supplemented with NCM (1 mg/mL), and subsequently adding it back to the spinner flask. On day 8, the culture medium was removed and replaced by a volume 1.5 times larger (NCM 1 mg/mL).

Before every medium change and at day 12, a 4 mL sample was collected from the spinner flask and digested

overnight (DMEM supplemented with 0.01% hyaluronidase and 0.2% collagenase A [Roche, Basel, Switzerland]) for determination of cell count and viability using the NucleoCounter (NC-100; ChemoMetec, Allerød, Denmark). During culture, chondrocytes and NCM assembled to form spherical organoids.

**2D expansion.** In addition, for each donor,  $1 \times 10^6$  viable chondrocytes were seeded in a T175 flask on day 0 and cultured in DMEM containing 10% FBS and 1% P/S at 37°C and 5% CO<sub>2</sub>. Medium was changed three times a week. On day 9, cells were passaged and their cell count was determined. On day 13, cells were harvested and cell count and viability were determined.

**Explant isolation.** On day 7, a second set of human tibial plateaus (6 subjects, 3 females and 3 males, aged  $70 \pm 13$  years, range 51–79 years) was collected. For every donor, three osteochondral explants (Ø 10 mm, bone length = 4 mm) were isolated from the tibial plateau covered by a smooth cartilage layer (for day 28 analysis) and two explants from areas with the least worn cartilage layer (for day 1 analysis). Explants were isolated using a custom-made trephine drill while cooling with sterile 4°C phosphate-buffered saline (PBS; Sigma-Aldrich) supplemented with 1% P/S. Full-depth chondral defects (Ø 6 mm) were created using a custom-made drill guide and a flat-bottomed drill bit. Explants were cultured at 37°C and 5% CO<sub>2</sub> in separate wells of a two-compartment culture system as described earlier and medium was refreshed every 2–3 days.<sup>6</sup>

The lower compartment contained 3 mL bone medium (DMEM supplemented with 10% FBS, 1% P/S, 25 µg/mL



fungin [InvivoGen, Toulouse, France], 50  $\mu\text{g}/\text{mL}$  L-ascorbic acid-2-phosphate, and 10 mM  $\beta$ -glycerophosphate [Sigma-Aldrich]) and the upper compartment contained 2.5 mL cartilage medium (DMEM supplemented with 1% P/S, 25  $\mu\text{g}/\text{mL}$  fungin, 40  $\mu\text{g}/\text{mL}$  L-proline [Sigma-Aldrich], 50  $\mu\text{g}/\text{mL}$  L-ascorbic acid-2-phosphate, and 1% ITS+ Premix).

Because of the timing of surgery, the explants were kept in culture for 6 days before defects were filled with implants. A pilot experiment showed that viable chondrocytes were still present throughout the cartilage and at the cut surfaces at this point. This was done using a 3-(4,5-dimethylthiazolyl-2)-2,5-diphenyltetrazoliumbromide (MTT; Invitrogen Molecular Probes, Eugene, OR) analysis. Samples were washed in PBS and incubated in 1 mL of 0.37 mg/mL MTT solution for 90 min at 37°C. Images were acquired

using a Keyence microscope (VHX-500FE, Osaka, Japan) and are shown in Figure 2.

**Implant formulation.** On day 13, the content of the spinner flasks was strained through a 70  $\mu\text{m}$  cell strainer to collect the organoids in the strainer. For each donor, organoids and 2D-cultured single cells were separately mixed into component I (fibrinogen component, diluted 1:15 in PBS<sup>16</sup>) of fibrin glue (Tisseel; Baxter, Deerfield, IL) at  $1 \times 10^6$  cells/80  $\mu\text{L}$  to form an organoid/fibrinogen and a cell/fibrinogen solution. Every chondrocyte donor from donor set 1 was randomly coupled to an explant donor of donor set 2 (one donor of donor set 1 was coupled to an extra explant donor of donor set 2 due to tissue availability). The edges of the defects in the explants were cleaned using a sharp spoon, and defects were blotted dry using sterile gauze.

Forty microliters of component II (thrombin component, diluted 1:50 in PBS<sup>16</sup>) was pipetted into the defect. Then, 80  $\mu\text{L}$  of the organoid/fibrinogen (two per donor) or cell/fibrinogen solution (two per donor) was added, followed by another 40  $\mu\text{L}$  of diluted component II, forming a fibrin clot containing the organoids or cells. For five donors, one defect was filled with cell-free fibrin (one for day 1 analysis, four for day 28 analysis) (Fig. 1). Subsequently, explants were incubated for 15 min at 37°C before fresh cartilage medium was added.

**Explant culture.** The explants containing the fibrin implants were cultured for 28 days at 37°C and 5% CO<sub>2</sub> and medium was changed every 2–3 days. After 1 day of culture, for every donor, one explant containing an organoid implant and one explant containing a cell implant were harvested (Fig. 1).

Using a 2-mm biopsy punch, a fibrin implant sample was removed from each defect for biochemical analysis (Fig. 1). These samples were weighed (wet weight) and stored at –80°C until use. Then, the cartilage of the explant was covered with a 3% agarose solution to restrict glycosaminoglycan (GAG) leakage and the explants were fixed in 3.7% formalin (Merck) for 24 h. The explants were then decalcified in a 12.5% ethylenediaminetetraacetic acid (EDTA; Sigma-Aldrich) solution at 37°C that was refreshed twice a week for 4 weeks.

After decalcification, the explants were stored in 3.7% formalin for 24 h and subsequently cut in half, dehydrated using a tissue processor (Microm, Walldorf, Germany), and embedded in paraffin (Paraplast; Sigma-Aldrich). For each explant, 10  $\mu\text{m}$  sections were prepared using a microtome (Leica, Wetzlar, Germany) and sections were stored at room temperature until further use.

**Histological examination and immunohistochemistry.** Sections of the osteochondral explants were stained for GAG and collagen with Safranin O/fast green (Sigma-Aldrich), and counterstained with Weigert's Iron Hematoxylin (Sigma-Aldrich). Collagen type II was visualized using the Vectastain avidin/biotin complex - alkaline phosphatase (ABC-AP) staining kit (Vector Laboratories, Burlingame, CA). In short, sections were treated with 0.05% pronase (30 min; Merck) followed by 0.5% hyaluronidase (30 min) and blocked with 0.05% PBS-Tween (Merck)/5% horse serum (Merck)/1% bovine serum albumin (Sigma-Aldrich) for 30 min.

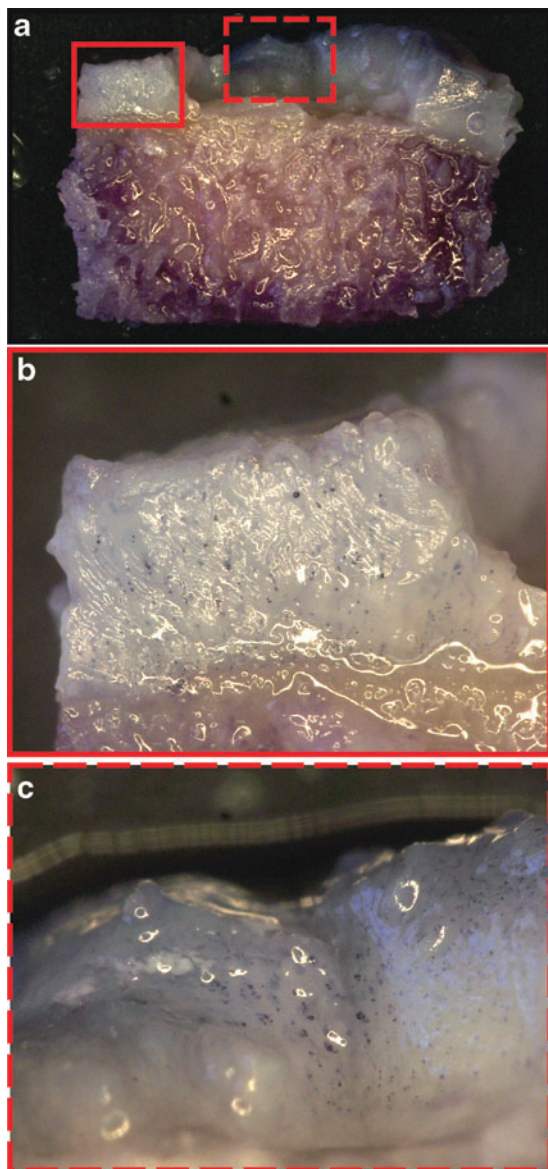


**FIG. 2.** MTT analysis showing the presence of viable cells after 6 days of culturing the explants with a defect before filling. (b, c) Magnifications of the areas indicated in red in (a). MTT, 3-(4,5-dimethylthiazolyl-2)-2,5-diphenyltetrazoliumbromide. Color images are available online.

Primary antibodies (II-II6B3, 1:100; Developmental Studies Hybridoma Bank, Iowa city, IA) were incubated overnight at 4°C. After incubation, samples were treated with a secondary antibody conjugated with Biotin (BA-2000, 1:200; Vector Laboratories) for 60 min. Thereafter, sections were incubated with the ABC-AP complex for 60 min and incubated with 5-bromo-4-chloro-3-indolyl phosphate (BCIP)/nitro blue tetrazolium (NBT) in demi-water (BCIP; SIGMAFAST/NBT; Sigma-Aldrich). Sections were counterstained with Nuclear Fast red (Sigma-Aldrich). All sections were visualized using Brightfield microscopy (Observer Z1; Carl Zeiss, Jena, Germany).

**Biochemical analysis.** Samples for biochemical analysis were lyophilized and weighed to determine their dry weight. Then samples were digested overnight at 60°C in papain digestion buffer (100 mM phosphate buffer, 5 mM L-cysteine, 5 mM EDTA, and 140 µg/mL papain, all from Sigma-Aldrich). Sulfated GAG (sGAG) content was determined using a dimethyl methylene blue assay with shark cartilage chondroitin sulfate (Merck) as a reference. The hydroxyproline (HYP) content, as measure for collagen content, was determined with a chloramine-T assay with a trans-4 HYP (Sigma-Aldrich) reference. DNA content was determined from the digested samples using the Qubit dsDNA high-sensitivity kit (Invitrogen, Waltham, MA) according to the manufacturer's instructions.

**Data analysis.** Data are presented as mean ± standard deviation. Statistical analysis was performed with Prism 9 (GraphPad Software, La Jolla, CA; www.graphpad.com). A Kruskal–Wallis test was conducted to examine the effect of culture duration on organoid and cell expansion, and if appropriate, a Dunn's *post hoc* test was done to discriminate between groups. Two-way analysis of variance (ANOVA) was performed to analyze the effect of culture time and implant type on the GAG, HYP, and DNA content of the organoid- and cell-filled implants (blocking for cell donor), and if appropriate, was followed by a Sidak's *post hoc* test. A Shapiro–Wilks test was used to check for normal distribution and a Brown–Forsythe test for homogeneity of variance. Statistical significance was assumed when  $p < 0.05$ .

### Experimental results

**Chondrocyte culture.** After the 3D spinner flask culture with NCM to induce organoid formation, the number of chondrocytes had significantly increased  $4.4 \pm 2.0$ -fold ( $p = 0.0045$ ) and viability was  $96.0\% \pm 1.7\%$  (Figs. 3a and 4a). In 2D, the number of chondrocytes had significantly increased  $5.4 \pm 1.6$ -fold ( $p = 0.0011$ ) and viability was  $98.3\% \pm 0.7\%$  (Figs. 3b and 4b).

**Tissue integration and regeneration in a human explant model.** Histological analysis of day 1 samples showed that organoids and single cells were evenly distributed throughout the gels in the defects (Fig. 5). Defects appeared to be macroscopically filled after 1 day of culture. After 28 days of culture, some defects were still filled to the surface, while in others the gel appeared to have contracted, often resulting from fibrin compaction and cells pulling on the gel. During the dehydration process before embedding the samples in paraffin, further shrinkage was not avoidable as the

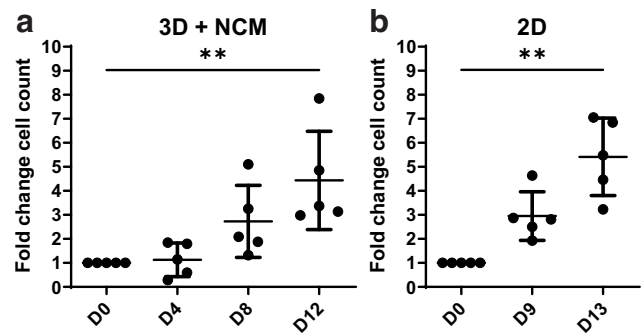


**FIG. 3.** Fold changes of the cell count for the spinner flask organoid culture with NCM (a) and the 2D cell culture (b). \*\* $p < 0.01$  NB: As cell counts for organoids require digestion, these were collected 1 day before end of culture (D13). NB, nota bene; NCM, notochordal cell-derived matrix. Color images are available online.

water was removed, resulting in the gels being separated from the native tissue in some locations.

Still, some interfaces remained intact, especially at the inner corners of the defects. It was observed that part of the gel remained attached to the native tissue, while the gel itself started tearing indicating that the adhesive strength was larger than the cohesive strength.

The organoids in the bottom and on the sides of the defect remodeled and merged, and cells migrated through the fibrin glue bridging the space between the organoids and between the organoids and the native cartilage. Newly formed tissue rich in proteoglycans was present in the organoid-filled and cell-filled defects, especially on the edges and in the corners (Figs. 6a–d and 7a–d). It was observed that in these proteoglycan-rich areas, the newly formed tissue integrated and interacted with the surrounding native cartilage, that is, cells and matrix crossing over the interface and cells were observed to reside in newly formed lacunae.

This integration was seen to some extent in all cell-containing constructs and did not differ between organoid- and cell-filled groups (organoids—4/6 at multiple locations and 2/6 only at one location; cells—4/6 at multiple locations and 2/6 only at one location). Toward the center of the implants, a fading proteoglycan gradient was observed. In organoid-containing constructs, the center of the implants

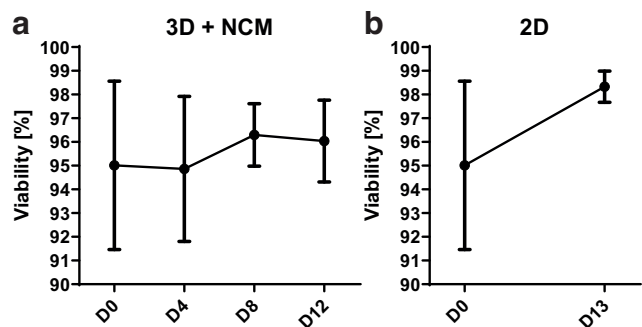


**FIG. 4.** Viability of the chondrocytes in the spinner flask organoid culture with NCM (a) and the 2D cell culture (b). NB: As cell counts for organoids require digestion, samples for %viability were also collected 1 day before end of culture (D13). Color images are available online.



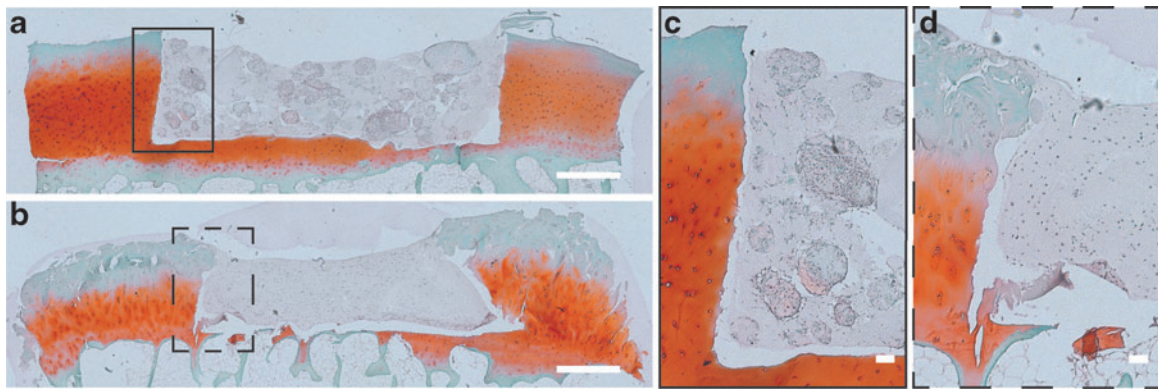


**FIG. 5.** Representative images of Safranin-O/fast green-stained sections of a defect filled with fibrin+organoids (**a, c**) and fibrin+cells (**b, d**) at day 1. Scale bar = 1000 μm for overview images and 100 μm for magnified views. Color images are available online.

showed less merging of organoids, and the cells present in this area had a different morphology (Fig. 6e).

Immunohistochemical analysis revealed the presence of collagen type II in the corner areas of both the organoid- and the cell-containing implants after 28 days, indicating limited dedifferentiation of the embedded chondrocytes (Figs. 6f and 7f). In explants filled with fibrin only, 3/4 constructs showed no integration or matrix production after 28 days of culture, with only a central fibrin clump detached from the adjacent tissue. For one construct, some contracted fibrin

was observed still attached to the adjacent tissue, and cell migration into the fibrin was observed with some proteoglycan- and collagen-containing matrix (Fig. 8).

**Biochemical analysis.** The GAG, HYP, and DNA content of the different implant types after 1 and 28 days of culture was compared (Fig. 9). Two-way ANOVA revealed that there were no statistically significant interactions between the effects of culture time and implant type for the GAG, HYP, and DNA content. Main effect analysis showed

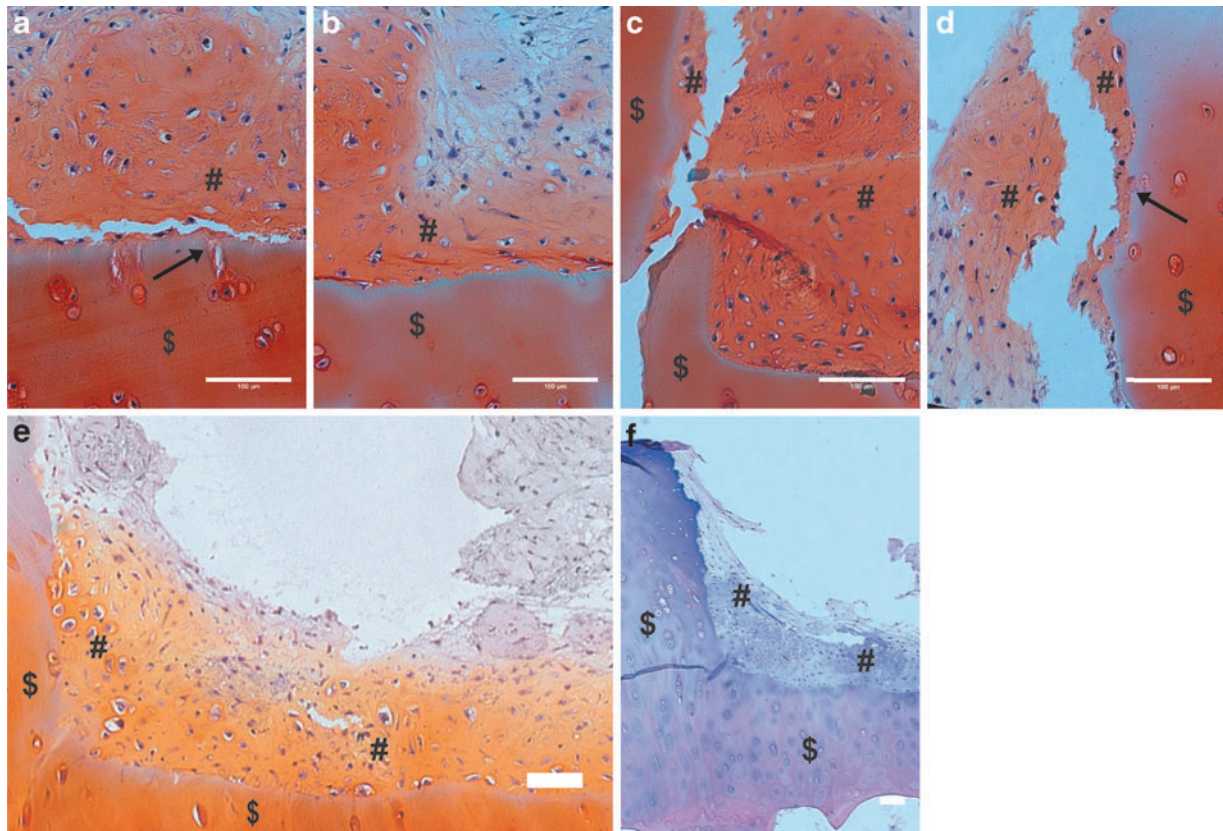


**FIG. 6.** Representative images of the *bottom* (**a–c**) and *lateral* (**c, d**) edges and the *corner* (**e**) of Safranin-O/fast green-stained sections and an immunohistochemical collagen type II-stained section (**f**) of defects filled with fibrin+organoids after 28 days of culture. #Fibrin implant; \$native cartilage, integration interaction depicted with *arrows*. Scale bar = 100 μm. Color images are available online.

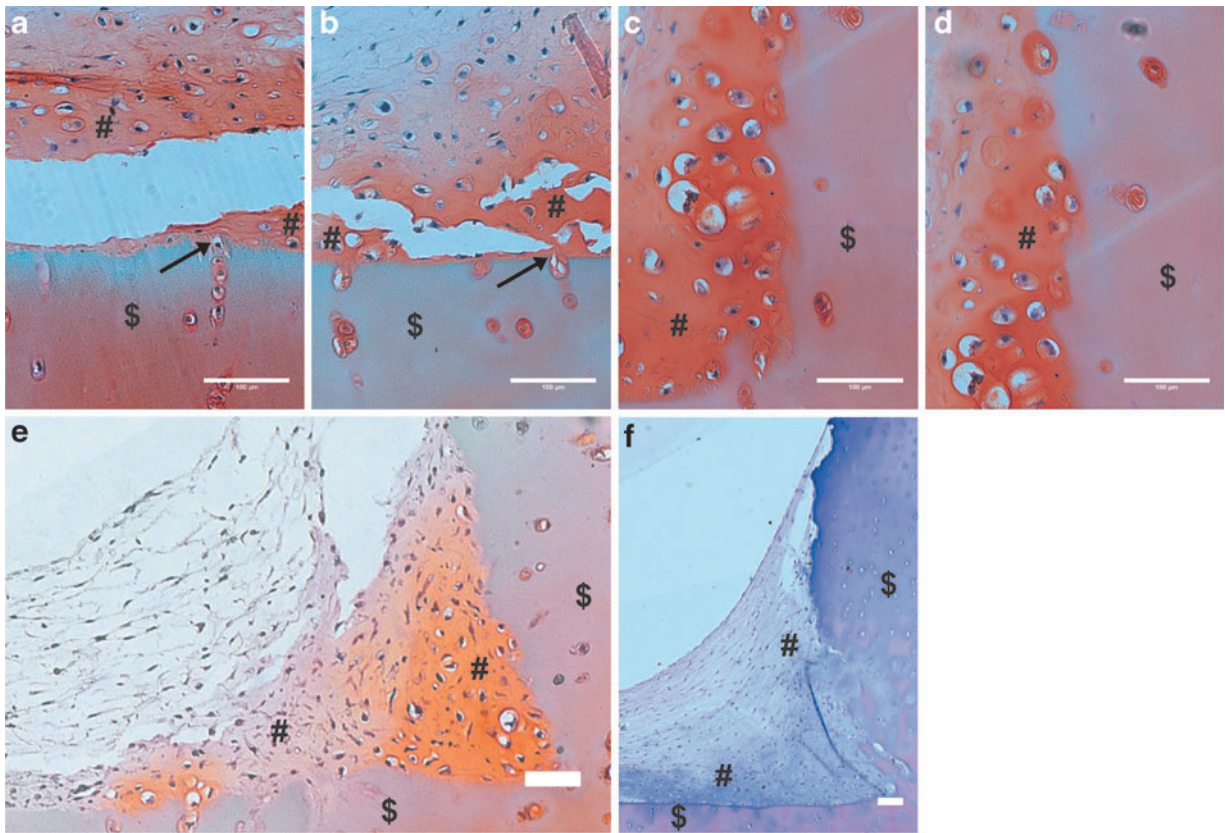


**FIG. 7.** Representative images of the *bottom* (a, b) and *lateral* (c, d) edges and the *corner* (e) of Safranin-O/fast green-stained sections and an immunohistochemical collagen type II-stained section (f) of defects filled with fibrin+cells after 28 days of culture. #Fibrin implant, \$native cartilage, integration interaction depicted with *arrows*. Scale bar=100  $\mu$ m. Color images are available online.

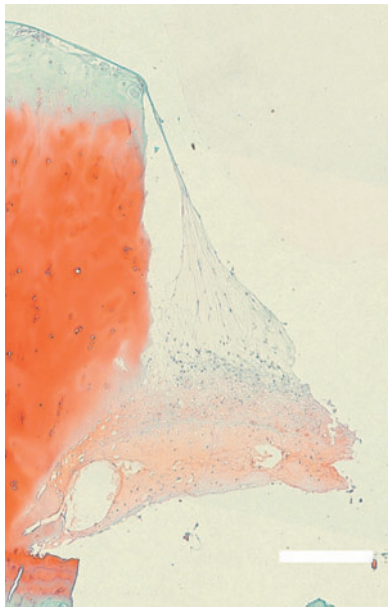


**FIG. 8.** Safranin-O/fast green-stained section of one of the defects filled with fibrin-only that showed some cell migration and production of extracellular matrix. Scale bar=500  $\mu$ m. Color images are available online.

a statistically significant effect of culture time on GAG content ( $p=0.010$ ), but only a trend for the different implant types ( $p=0.074$ ).

*Post hoc* analysis showed a nearly significant ( $p=0.079$ ) increase in GAG from day 1 to day 28 for the organoid-filled implants. For HYP content, main effect analysis indicated a statistically significant effect of implant type ( $p=0.002$ ), but not of culture time ( $p=0.199$ ). *Post hoc* analysis showed a higher HYP content in organoid-filled implants compared with cell-filled implants both at day 1 ( $p=0.002$ ) and at day 28 ( $p=0.002$ ). No statistically significant effect of culture time ( $p=0.419$ ) nor implant type ( $p=0.946$ ) was found for the DNA content of the implants.

#### *Institutional Review Board/Animal Care and Use Committee approval*

The Medical Ethics Committee Máxima Medisch Centrum declared that the rules laid down in Medical Research Involving Human Subjects Acts [in Dutch] [wet medisch wetenschappelijk onderzoek met mensen (WMO)] do not apply to this project. The Institutional Review Board approved the execution of this project (N16.148).

#### **Discussion**

Integration of a tissue-engineered implant with the surrounding native cartilage is crucial for cartilage repair. It



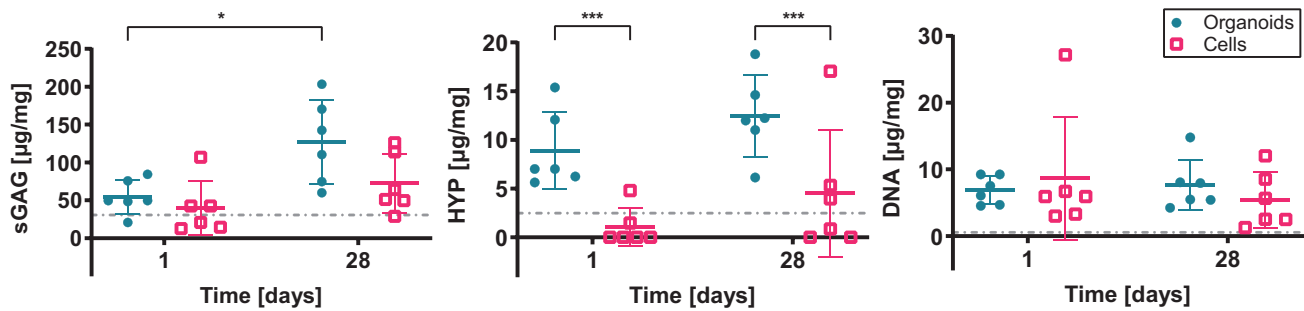


**FIG. 9.** sGAG, HYP, and DNA content (mean  $\pm$  SD) of the organoid- and cell-filled fibrin implants after 1 and 28 days of culture. The content of the fibrin-only implants after 28 days was added as a reference line in gray (mean, SD = 35.70, 4.287, and 0.8408  $\mu$ g/mg for sGAG, HYP, and DNA, respectively). One fibrin-only sample was covered by cartilage and thus was not used in the biochemical analysis. Significant  $p$ -values for ANOVA main factors are not shown in the graphs (culture time [sGAG\*\*], implant type [sGAG\* and HYP\*\*\*]). Significant  $p$ -values were indicated for *post hoc* tests: \* $p$  < 0.08, \*\* $p$  < 0.05, and \*\*\* $p$  < 0.01. ANOVA, analysis of variance; HYP, hydroxyproline; sGAG, sulfated glycosaminoglycan. Color images are available online.

accounts for a better load distribution within the joint and strengthens the border of the original defect, thereby reducing the risk for future cartilage deterioration.<sup>4</sup> In the present study, it was shown that the *ex vivo* human osteochondral explant culture model can be used to demonstrate integration between an organoid- or cell-laden fibrin implant and native cartilage from osteoarthritic patients (Figs. 6 and 7). It is hypothesized that the initial integration observed is indicative for integration *in vivo* in patients because of the species-specific surrounding cartilage and bone tissue.

A full representation of the *in vivo* situation is, however, not possible due to the absence of various factors such as physiological loading, other joint tissues, the immune interactions, and systemic factors acting through the blood circulation. Obviously, also *in vivo* there may be a large variation in the rate of matrix development and integration between disease severity and/or patients, and the anabolic rate in the present *ex vivo* model may be on the fast or slow end of the spectrum. A direct comparison with *in vivo* results is difficult as there are no histological data at the 28-day time point in humans.

Because the tissues are species specific and the direct environment is similar, it is, however, believed that this model is indicative of initial implant integration and could be useful to explore enhancement thereof, for example, by modulating gel properties, incorporating slow-releasing drugs, pretreating defect edges, or altering cell source before proceeding to animal experimentation.

Integration and interaction of the implants with the surrounding cartilage were observed at the bottom and lateral sides of the defects, where cells show a chondrocyte-like round morphology. Histology showed that GAGs and collagen were not equally distributed throughout the tissue but were mainly present near the cartilage explant interface in the gel, and predominantly in the corners deeper in the defects (Figs. 6 and 7). Similar integration and matrix distribution were observed in a study in which pig chondrocytes were embedded in an *ex vivo* chondral defect within human cartilage explants and using bovine cells in bovine osteochondral explants.<sup>17,18</sup>

Although GAGs and collagen could have been only produced near the interfaces, alternatively, matrix could have been produced throughout the implant, then diffused out of the fibrin glue and only remained where it could attach to a significant matrix that was already formed.<sup>19,20</sup> This would

indicate that visible matrix accumulation starts near the edges, and then slowly grows over time, starting from the corners where there are two sides of native ECM nearby, until there is matrix everywhere.

Biochemical analysis showed a statistically significant effect of culture time on GAG content and it was shown that the HYP content was significantly higher in organoid-filled implants compared with cell-filled implants at both time points. From these data it seems that for cell-filled implants, the GAG and HYP content did not increase much during culture, but in organoid-filled implants the GAG content increased more almost beyond the variance within the individual donors. The organoid-filled implants already started with a greater HYP content initially (having produced/ incorporated much during their self-assembly during expansion) and maintained this during culture relative to that of the cell-filled implants.

Therefore, after 28 days of culture, the organoid-filled implants tended to have a higher GAG and HYP content compared with the cell-filled implants, which may be beneficial for early load bearing and mechanical stimulation. However, a limitation of this analysis is that the complete data set was not normally distributed. The Shapiro–Wilk normality test was not passed for all groups (day 1 organoids' GAG [ $p$  < 0.04], day 1 and day 28 cells' HYP [ $p$  < 0.01 and  $p$  < 0.03, respectively], and day 1 cells' DNA [ $p$  < 0.01]). This was probably because the sample size per group was too small due to the limited availability of human tissue.

As there is no equivalent two-way blocked nonparametric analysis available, the data were only partially somewhat non-normal, and ANOVAs are rather robust to non-normality, it was decided to present the two-way ANOVA, keeping in mind that these results are simply indicators and that further studies are required to investigate the advantages of organoid-based cartilage implants. Nevertheless, these results are in agreement with what was histologically observed, where proteoglycan and collagen increased in the implants during 28 days of culture.

Another plausible explanation for the small (nonsignificant) increase measured in the GAG and HYP content during 28 days of culture is the location of sample extraction. The  $\emptyset$  2 mm sample that was extracted for biochemical analysis might not have contained the GAG- and collagen-rich matrix that was mainly observed in the corners of the defects.

Longer culture times are likely to lead to a more pronounced increase in GAG and HYP content, filling the gel from the corners toward the center. However, in this proof-of-principle study, the culture time was limited to 28 days as the stability of the human explant culture model used in this study was only validated for this culture duration.<sup>6,21</sup>

A volume loss of the fibrin implants was observed during culture, resulting in an incomplete defect-fill. This was worst in the cell-filled implants, but also seen to some extent in some of the organoid-filled implants. Diluted fibrin was used according to the protocol of Abbadessa *et al.*, who also observed compaction of the fibrin during the first days of culture.<sup>16</sup> The compaction of fibrin gels has been described earlier in literature.<sup>22,23</sup> Sage *et al.* observed that when using cartilage chips, the shape and size of the fibrin gels were more stable.<sup>24</sup>

A similar observation was made in the present study when mixing the fibrin with matrix-containing organoids compared with single cells. Due to the advantage for clinical use, the Tisseel fibrin glue was used. An alternative would be to prepare the fibrin gel from chemicals that are research-use only. Eyrich *et al.* described the formation of a fibrin gel that was more stable in shape and volume and also promoted GAG and collagen formation in the gel.<sup>23</sup> Processing of the constructs for paraffin embedding and sectioning might have contributed to more shrinkage and tearing of the gels,<sup>25</sup> partly separating them from the native cartilage, as shown in the histology images. Some interfaces were, however, preserved, revealing integration between the implant and the native cartilage.

Due to the contractive properties of the fibrin-based implants and the additional difficulties in processing the samples for histology, the ability to show the sensitivity of the model to discern between integration of the two different cell-based fibrin implants in this study was limited. Optimized sample processing and the use of a less contractive carrier material might affect the amount of integration seen in histological sections, thereby increasing the value of histological analysis.

Future experiments could also include additional non-destructive methods to quantitatively assess tissue quality and integration between implants and the surrounding tissue, for example, magnetic resonance imaging or ultrasound imaging.<sup>26–28</sup> Push-out tests could provide quantitative information on the integration strength between interfaces, although this would only assess lateral integration strength.<sup>4,29</sup>

The donor tissue used for this study was obtained from TKR surgeries of osteoarthritic patients between 51 and 79 years old. It is well known that age plays a role in the metabolic activity and proliferative capacity of chondrocytes.<sup>7,30</sup> Ideally, tissue of younger individuals would be used, as that would have been more representative for the patient population that receives regenerative treatments. However, the setup of this study required four or five explants per patient, which requires a large joint surface. Considering ethical and practical issues, this could only be obtained from a human residual tissue available after TKR surgery, which is rare in young patients.

Even though the tissue formation and integration observed in this study are likely low compared with that in younger patients with superior regenerative capacity, using

the older human tissue was preferred above using tissue from an animal source as it has some major advantages.

First, research has shown that species variability in chondrocyte expansion and differentiation potential restrict predictive cartilage repair studies in animal models.<sup>5</sup> In the final application it is likely that a patients' own cells will be used, so by using human patient tissue, the need to discuss or compensate for structural, compositional, and species-specific differences is reduced.<sup>18,30,31</sup>

Second, the use of this patient tissue eliminates the need for inducing early OA conditions in an artificial way, contributing to a model that is more representative for the natural disease. In addition, the use of this human tissue also represents the variability between and within patients. This makes it more difficult to retrieve unambiguous results and therefore significant differences between the various conditions, yet it does represent a spectrum of patients suffering from focal cartilage defects.

Compared with other spheroid techniques that require *in vitro* 2D expansion of chondrocytes before moving to 3D culture of the cells, the current spinner flask chondrocyte culture combines expansion and organoid formation into one step, preventing the primary chondrocytes from dedifferentiation during 2D culture and reducing the time needed for culturing.<sup>11–13,15</sup> Remodeling and merging of the organoids were comparable with studies described in literature.<sup>11,32</sup>

Clinically, the use of porcine NCM leads to challenges such as disease transmission and batch-to-batch variability. To this extent, it is important to study and identify the ECM molecules and (growth)factors in the NCM that are important for the generation of cartilage organoids. Once unraveled, a synthetic cocktail might be developed that could replace the porcine NCM for clinical purposes. Another possibility is to further process the porcine NCM for *in vivo* applications.<sup>33–35</sup>

In conclusion, this human culture model can be used to test and identify promising implant strategies through *ex vivo* evaluation of integration and matrix production, leading to a decrease in animal experimentation. Nevertheless, *in vivo* animal trials will continue to be a part of the implant design trajectory, as *ex vivo* models lack the influence of systemic factors, immune response, and physiological load. Expanding the *ex vivo* model by adding mechanical loading, coculturing different cell types, or adding cytokines might add more complexity to the model, allowing for a more complete evaluation in an earlier stage of development, and therefore, a further decrease in the number of animal studies and/or entering clinical trials with more detailed knowledge of potential implant behavior.

#### Authors' Contributions

M.W.A.K. designed and conducted the experiments, interpreted and analyzed the data, and wrote the article. C.C.v.D. and K.I. secured the funding, contributed to the experiment design, data interpretation, and article review. R.P.A.J. contributed to tissue procurement and harvesting as well as data interpretation and article review. J.F.C. provided expertise with the organoid production and analysis and contributed to data interpretation and article review. All authors have read and approved the final submitted article.

### Acknowledgments

The authors thank LifeTec Group and, in particular, Linda Kock for providing support using the culture platforms. The authors also thank Marieke C. van der Steen for her help in the METC approval for the use of human osteochondral tissue.

### Disclosure Statement

M.W.A.K., J.F.C., C.C.v.D., and R.P.A.J.: No competing financial interests exist. K.I. is contracted as CSO of NC Biomatrix BV and is a silent shareholder in the company.

### Funding Information

This article is supported by the partners of Regenerative Medicine Crossing Borders (RegMed XB), a public/private partnership that uses regenerative medicine strategies to cure common chronic diseases. This collaboration project is financed by the Dutch Ministry of Economic Affairs by means of the PPP Allowance made available by the Top Sector Life Sciences and Health to stimulate public/private partnerships.

### References

- Sophia Fox, A.J., Bedi, A., and Rodeo, S.A. The basic science of articular cartilage: structure, composition, and function. *Sport Health* **1**, 461, 2009.
- Stampoultzis, T., Karami, P., and Pioletti, D.P. Thoughts on cartilage tissue engineering: a 21st century perspective. *Curr Res Transl Med* **69**, 103299, 2021.
- Armiento, A.R., Alini, M., and Stoddart, M.J. Articular fibrocartilage—why does hyaline cartilage fail to repair? *Adv Drug Deliv Rev* **146**, 289, 2019.
- Trengove, A., Di Bella, C., and O'Connor, A.J. The challenge of cartilage integration: understanding a major barrier to chondral repair. *Tissue Eng Part B Rev* 2021. doi: 10.1089/ten.teb.2020.0244.
- Giannoni, P., Crovace, A., Malpeli, M., *et al.* Species variability in the differentiation potential of in vitro -expanded articular chondrocytes restricts predictive studies on cartilage repair using animal models. *Tissue Eng* **11**, 237, 2005.
- Kleuskens MWA, Donkelaar, C.C., Kock, L.M., *et al.* An ex vivo human osteochondral culture model. *J Orthop Res* **39**, 871, 2021.
- Barbero, A., Grogan, S., Schäfer, D., *et al.* Age related changes in human articular chondrocyte yield, proliferation and post-expansion chondrogenic capacity. *Osteoarthritis Cartilage* **12**, 476, 2004.
- Schulze-Tanzil, G., De Souza, P., Villegas Castrejon, H., *et al.* Redifferentiation of dedifferentiated human chondrocytes in high-density cultures. *Cell Tissue Res* **308**, 371, 2002.
- Yan, H., and Yu, C. Repair of full-thickness cartilage defects with cells of different origin in a rabbit model. *Arthroscopy* **23**, 178, 2007.
- Caron, M.M.J., Emans, P.J., Coolen, M.M.E., *et al.* Redifferentiation of dedifferentiated human articular chondrocytes: comparison of 2D and 3D cultures. *Osteoarthritis Cartil* **20**, 1170, 2012.
- Anderer, U., and Libera, J. In vitro engineering of human autogenous cartilage. *J Bone Miner Res* **17**, 1420, 2002.
- Schubert, T., Anders, S., Neumann, E., *et al.* Long-term effects of chondrospheres on cartilage lesions in an autologous chondrocyte implantation model as investigated in the SCID mouse model. *Int J Mol Med* **23**, 455, 2009.
- Meyer, U., Wiesmann, H.P., Libera, J., *et al.* Cartilage defect regeneration by ex vivo engineered autologous microtissue—preliminary results. *In Vivo* **26**, 251, 2012.
- De Vries, S.A.H., Van Doeselaar, M., Kaper, H.J., *et al.* Notochordal cell matrix as a bioactive lubricant for the osteoarthritic joint. *Sci Rep* **8**, 1, 2018.
- Crispim, J.F., and Ito, K. De novo neo-hyaline-cartilage from bovine organoids in viscoelastic hydrogels. *Acta Biomater* **128**, 236, 2021.
- Abbadessa, A., Mouser, V.H.M., Blokzijl, M.M., *et al.* A synthetic thermosensitive hydrogel for cartilage bioprinting and its biofunctionalization with polysaccharides. *Biomacromolecules* **17**, 2137, 2016.
- Fuentes-Boquete, I., Lopez-Armada, M.J., Maneiro, E., *et al.* Pig chondrocyte xenografts for human chondral defect repair: an in vitro model. *Wound Repair Regen* **12**, 444, 2004.
- de Vries-van Melle, M.L., Mandl, E.W., Kops, N., *et al.* An osteochondral culture model to study mechanisms involved in articular cartilage repair. *Tissue Eng Part C Methods* **18**, 45, 2012.
- Li, Z., Yao, S.-J., Alini, M., *et al.* Chondrogenesis of human bone marrow mesenchymal stem cells in fibrin-polyurethane composites is modulated by frequency and amplitude of dynamic compression and shear stress. *Tissue Eng Part A* **16**, 575, 2010.
- Iseki, T., Rothrauff, B.B., Kihara, S., *et al.* Dynamic compressive loading improves cartilage repair in an in vitro model of microfracture: comparison of 2 mechanical loading regimens on simulated microfracture based on fibrin gel scaffolds encapsulating connective tissue progenitor cells. *Am J Sports Med* **47**, 2188, 2019.
- Mouser, V.H.M., Dautzenberg, N.M.M., Levato, R., *et al.* Ex vivo model unravelling cell distribution effect in hydrogels for cartilage repair. *ALTEX* **35**, 65, 2018.
- Ahmed, T.A.E., Dare, E.V., and Hincke, M. Fibrin: a versatile scaffold for tissue engineering applications. *Tissue Eng Part B Rev* **14**, 199, 2008.
- Eyrich, D., Brandl, F., Appel, B., *et al.* Long-term stable fibrin gels for cartilage engineering. *Biomaterials* **28**, 55, 2007.
- Sage, A., Chang, A.A., Schumacher, B.L., *et al.* Cartilage outgrowth in fibrin scaffolds. *Am J Rhinol Allergy* **23**, 486, 2009.
- Duchi, S., Doyle, S., Eekel, T., *et al.* Protocols for culturing and imaging a human ex vivo osteochondral model for cartilage biomanufacturing applications. *Materials (Basel)* **12**, 640, 2019.
- Trattinig, S., Winalski, C.S., Marlovits, S., *et al.* Magnetic resonance imaging of cartilage repair: a review. *Cartilage* **2**, 5, 2011.
- Schöne, M., Männicke, N., Somerson, J.S., *et al.* 3D ultrasound biomicroscopy for assessment of cartilage repair tissue: volumetric characterisation and correlation to established classification systems. *Eur Cell Mater* **31**, 119, 2016.
- Pastrama, M., Spierings, J., van Hugten, P., *et al.* Ultrasound-based quantification of cartilage damage after in vivo articulation with metal implants. *Cartilage* **13**, 1540S, 2021.



29. van de Breevaart Bravenboer, J., In der Maur, C.D., Bos, P.K., *et al.* Improved cartilage integration and interfacial strength after enzymatic treatment in a cartilage transplantation model. *Arthritis Res Ther* **6**, R469, 2004.
30. Li, Y., Wei, X., Zhou, J., *et al.* The age-related changes in cartilage and osteoarthritis. *Biomed Res Int* **2013**, 916530, 2013.
31. Schwab, A., Meeuwssen, A., Ehlicke, F., *et al.* Ex vivo culture platform for assessment of cartilage repair treatment strategies. *ALTEX* **34**, 267, 2017.
32. Bartz, C., Meixner, M., Gieseemann, P., *et al.* An ex vivo human cartilage repair model to evaluate the potency of a cartilage cell transplant. *J Transl Med* **14**, 2016.
33. Wong, M.L., and Griffiths, L.G. Immunogenicity in xenogenic scaffold generation: antigen removal vs. decellularization. *Acta Biomater* **10**, 1806, 2014.
34. Illien-Jünger, S., Sedaghatpour, D.D., Laudier, D.M., *et al.* Development of a bovine decellularized extracellular matrix-biomaterial for nucleus pulposus regeneration. *J Orthop Res* **34**, 876, 2016.
35. Gilbert, T.W., Sellaro, T.L., and Badylak, S.F. Decellularization of tissues and organs. *Biomaterials* **27**, 3675, 2006.

Address correspondence to:  
*Corrinus C. van Donkelaar, PhD*  
*Orthopaedic Biomechanics*  
*Department of Biomedical Engineering*  
*Eindhoven University of Technology*  
*Gemini Zuid 1.106, PO Box 513*  
*Eindhoven 5600 MB*  
*The Netherlands*

*E-mail: c.c.v.donkelaar@tue.nl*

*Received: October 26, 2021*

*Accepted: January 3, 2022*

*Online Publication Date: January 17, 2022*